ELSEVIER

Int. J. Therm. Sci. 41 (2002) 586–598

International Journal of Thermal Sciences

www.elsevier.com/locate/ijts

Experimental studies of boiling mechanisms in all boiling regimes under steady-state and transient conditions ☆

Hein Auracher [a,*], Wolfgang Marquardt [b]

[a] *TU Berlin, Institut für Energietechnik, Sekr. KT1, Marchstr. 18, D-10587 Berlin, Germany*
[b] *RWTH Aachen, Lehrstuhl für Prozesstechnik, Turmstr. 46, 52064 Aachen, Germany*

Received 29 October 2001; accepted 8 February 2002

Abstract

The paper presents a summary of results found in the first author's laboratories during recent years. First an experimental technique suitable for precise and systematic measurements of entire boiling curves under steady-state and transient conditions is described. The experimental results for pool boiling of well wetting fluids and fluids with a larger contact angle (FC-72, isopropanol, water) show no evidence of a hysteresis in the transition region if the heater surface is clean. For a surface with contamination, however, the boiling curves are not reproducible. The situation is different under transient conditions: heating and cooling transients yield different curves. Boiling experiments with a water jet impinging vertically on a hot surface show similar boiling mechanisms as in pool or forced convective boiling except for the transition region, but the heat fluxes are significantly larger. In the transition region very large heat fluxes are observed until a rather abrupt transition to film boiling at very high wall superheats. Measurements with a micro-optical probe give a detailed insight in the behavior of the macrolayer in the different boiling regimes. Temperature signals from microthermocouples very near the heater surface and the optical probe data lead to some conclusions on the physics of boiling in the different boiling regimes. In particular it was found that convective effects in the boundary layer are probably responsible for the deviations between transient and steady-state boiling heat transfer.

Keywords: Pool boiling; Jet impingement; Boiling curve; Transient boiling; Transition boiling; Hysteresis; Optical probes; Macrolayer

1. Introduction

Despite of the enormous number of studies on boiling heat transfer we still have far more empirical results than knowledge on the physical mechanisms. Empirical correlations required for design purposes in practice still govern the field. But it is now accepted that further progress requires emphasis on studies focused on the physics of this very complex process. This trend is on one hand supported by new experiments—which are doubtless unavoidable in this field—taking advantage of the growing capacities in data processing by computers in connection with miniaturized sensors and high speed cinematography and other optoelectronic facilities, and on the other by better and new mathematical tools which have been developed in recent years.

The objective of the present report is to present a summary of results found in our laboratories during the past years. Most of these results have already been published elsewhere (e.g., [1–7]). The philosophy of our research follows the lines mentioned above.

In the first and second part a novel experimental technique is presented which enables a precise and systematic measurement of entire boiling curves under steady-state and transient conditions. This technique has been applied, in the first step, to find out whether boiling curves exhibit a hysteresis in the transition region under steady-state conditions. There are still controversial opinions about this aspect. To find an answer, steady-state experiments were carried out with well wetting fluids and fluids with a larger contact angle (FC-72, isopropanol, water). Moreover, boiling curves under transient heating and cooling conditions have been determined with FC-72. Here, the heating and cooling rate could be varied systematically. Also jet impingement experiments with water are presented. With the same technique, boiling

☆ This article is a follow-up a communication presented by the authors at the ExHFT-5 (5th World Conference on Experimental Heat Transfer, Fluid Mechanics and Thermodynamics), held in Thessaloniki in September 24–28, 2001.

* Correspondence and reprints.
E-mail addresses: auracher@iet.tu-berlin.de (H. Auracher), marquardt@lfpt.rwth-aachen.de (W. Marquardt).

1290-0729/02/$ – see front matter
PII: S1290-0729(02)01352-2

Nomenclature

p	pressure ..... MPa	*Subscripts*	
x	distance from the stagnation line ..... mm	cr	critical
ΔT	$= T_w - T_s$ wall superheat ..... K	s	saturation
		w	wall

curves have been obtained for steady-state conditions inside and outside of the stagnation region.

A precise technique to determine entire boiling curves is a necessary prerequisite to study the boiling mechanisms in the different boiling regimes. Results of this kind are presented in the third part of our report. A micro-optical probe was applied to study the two-phase behaviour above the heating surface in the different boiling regions. Microthermocouples beneath the surface were used to measure temperature fluctuations due to the action of the two-phase system above the surface. All the obtained results lead to some interesting conclusions on the physics of boiling in the different boiling regimes.

2. Experimental facilities

2.1. Test loops

An outline of the test loop for pool boiling experiments is shown in Fig. 1. The main components are the boiling vessel (diameter 209 mm, height 332 mm), the vapor generator and the condenser. The maximum operating pressure of the test loop is 1.0 MPa. In the water and isopropanol tests, the vapor generator provides a basic load for the condenser. It also reheats potentially subcooled liquid from the condenser to preserve constant saturation state at the boiling vessel inlet. The condenser is cooled with Thermogen 1693 (Clariant Company), a synthetic heat transfer fluid. An electric heater and a heat exchanger, both temperature controlled, realize constant inlet conditions. A recirculated thermostatic bath B filled with Thermogen 1693 is used to keep constant saturation conditions in the boiling vessel via two tube coils.

In tests with FC-72 the condenser and the thermostatic bath B are cooled with water. A separate vapor generator is not necessary here. A filter loop with a heat exchanger, a hermetic pump and a filter with an absolute removal rating of 1 μm can be used to remove small particles from the test fluid. Four sightglasses at heater level and two at an angle of 45° allow observation of the boiling process. An optical probe can be installed from the top of the boiling vessel and moved in xyz-direction by a micrometer-adjusting device. The test loop is completely made from stainless steel, pickled, electropolished and passivated.

The test loop for the jet impingement cooling experiments with water is similar to the one shown in Fig. 1. Details are presented in [1]. All the test runs have been carried out at atmospheric pressure with a subcooled free jet vertically directed to a horizontal heater (Fig. 4) fixed at the bottom of a boiling vessel similar to the one in Fig. 1.

2.2. Test heaters

Pool boiling experiments with water and isopropanol. A scheme of the heater section is shown in Fig. 2. The test heater with a boiling surface diameter of 35 mm and a thickness of 8 mm is installed in a stainless steel housing. The test heater is made of high purity copper. It is cylindrical in the top part and quadratic in the bottom part with the edges cut off (see [2] for more details). The quadratic shape of the bottom part is necessary for the chosen heating technique, see below. A cover of the hydrolysis resistant synthetic PEEK on the housing limits boiling at the top of the heater and reduces heat losses to the environment.

Heat input is provided by means of electric resistance heating through a 25 μm thick heating foil with a specific resistance of 108 μΩ·cm. The foil is pressed onto the bottom of the heater with a sheet of aluminiumnitride ceramic in between for electrical insulation to the heater. The bended connectors of the heating foil consist of a different material with a low electrical resistance to prevent burnout of the foil outside the test heater. The maximum design heat flux of the test heater is 5.5 $MW \cdot m^{-2}$ with a maximum heating current of 350 A.

Four thermocouples (type K) with a diameter of 0.25 mm were implanted inside the heater by an electroplating process. This technique allows the installation of thermocouples parallel to the heating surface. The sensitive tips are located 1.3 mm below the surface. The thermocouples are used for the control of the heater surface temperature, for evaluation of the boiling curve, and for overtemperature protection.

The boiling surface is protected against corrosion with a nickel layer of approximately 50 μm thickness. The nickel was deposited on the test heater by an electroplating process. The surface was finished with P2000 emery paper and cleaned with acetone and distilled water.

Pool boiling experiments with FC-72. Two heaters are used for the experiments with FC-72 (C_6F_{14}, 3-M company), one for steady-state and the other for transient experiments. They are similar except for the size and the heating mode. For steady-state experiments a copper heater (No. 1) with 34 mm

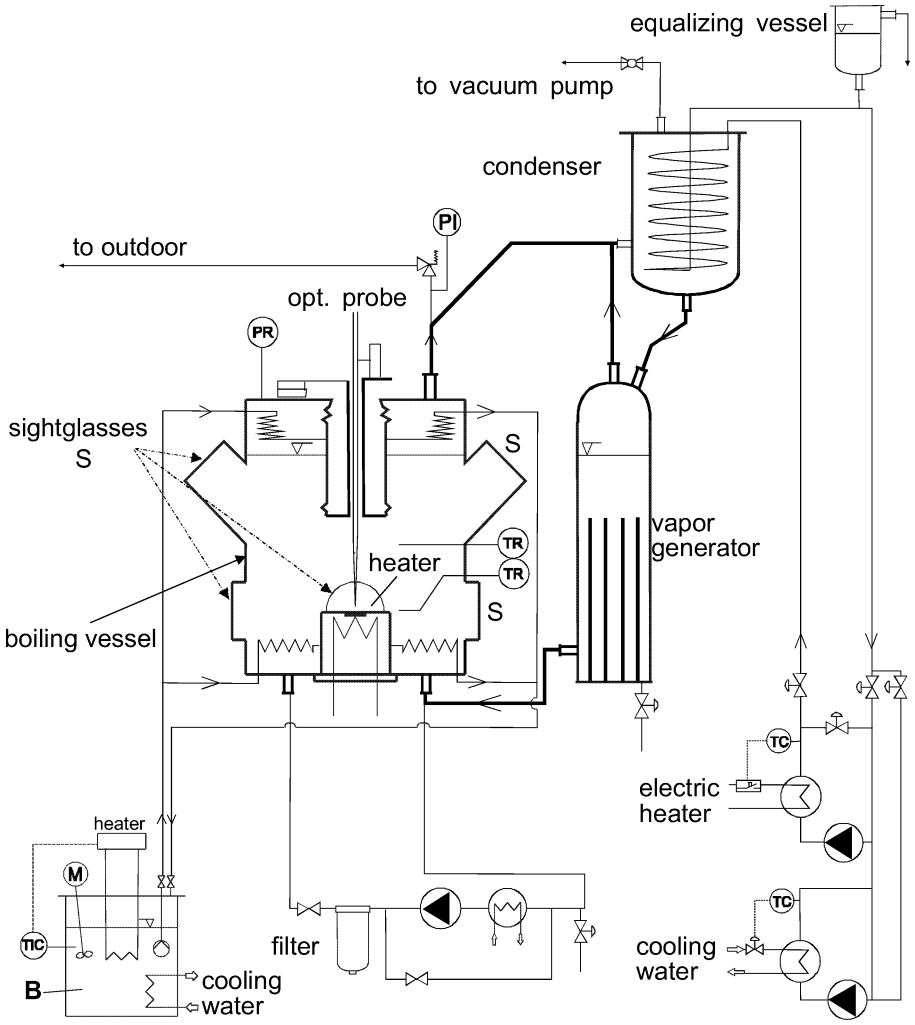

Fig. 1. Outline of the test loop.

diameter and 10 mm thickness, DC-heated indirectly from the bottom by a sheathed resistance wire, was applied. For more details see, e.g., [3]. For transient experiments a heater (No. 2) with lower thermal inertia and higher maximum heat input was used (Fig. 3). The design of this heater is similar to the one used for the water and isopropanol experiments (Fig. 2). It consists of a 5 mm thick copper block, 20×20 mm squared in the bottom part and cylindrical with 18.2 mm diameter in the top part. It is insulated ($\lambda = 0.22\ \mathrm{W{\cdot}m^{-1}{\cdot}K^{-1}}$) and sealed by polyimide.

Heat losses through the polyimide block are small, hence one-dimensional heat conduction can be assumed. Heating is accomplished by DC (20 V, max. 200 A) flowing through a foil made of a titanium/aluminium/vanadium alloy (thickness: 12.5 μm, spec. electric resistance: 126 μΩ·cm). The foil is pressed to the bottom of the heater with a 0.025 mm thick plate of muscowite mica in between for electrical insulation. The surface of the heater is electroplated with a 20 μm nickel-layer. Three thermocouples of 0.25 mm outer diameter are implanted 1.3 mm beneath the heating surface by electroplating. One is used as sensor for temperature control, one as safety sensor against overheating and one to determine the surface temperature. A number of microthermocouples to measure the surface temperature fluctuations are also installed in heater No. 2 (for details see [4]).

Jet impingement experiments with water. This test heater is made from a single piece of pure copper, divided into 8 sections by small slots of 3.8 mm depth (Fig. 4). Each section is heated from the bottom and independently temperature controlled. The individual heaters have a surface area of $10 \times 10\ \mathrm{mm^2}$. The jet with an outlet cross sectional area of $1 \times 9\ \mathrm{mm^2}$ impinges at the centre of the second heater and flows along the heater cascade in an open channel formed by a ceramic plate (for more details of the jet impingement experiments see [1]). The non-evaporated part of the water is drained off through discharge tubes (A, Fig. 4). To avoid heat losses, Sections 1 and 8 are used as guard heaters. Therefore, heat transfer evaluations are only carried out for heaters 2 to 7. Hence, results are obtained for the region between the stagnation line ($x = 0$) up to a distance of 55 mm to it.

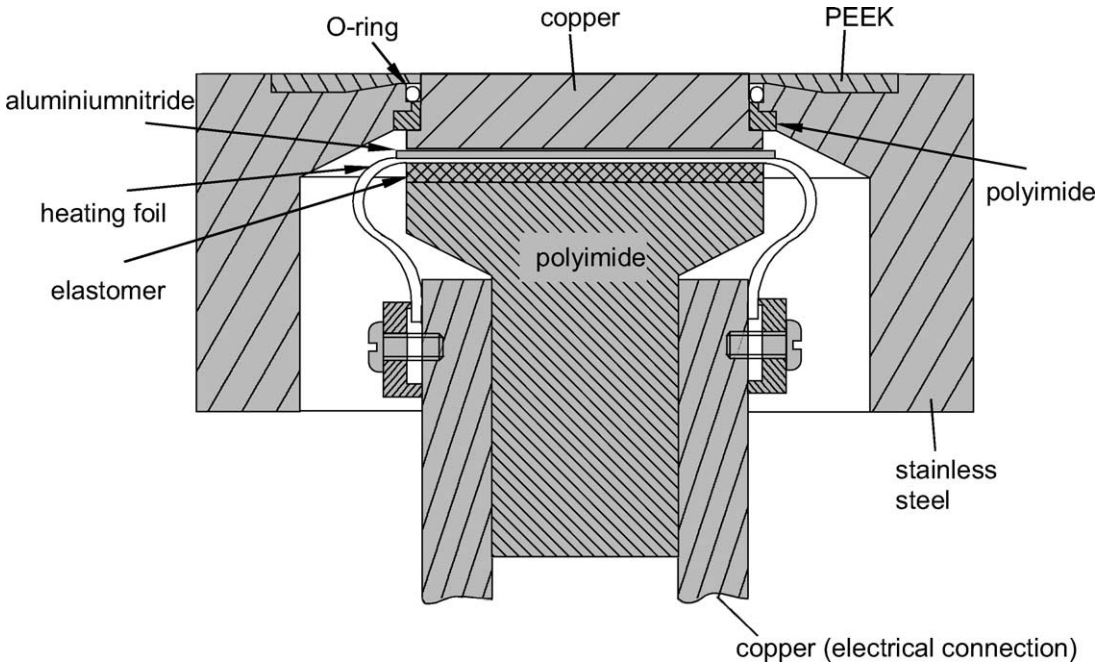

Fig. 2. Scheme of upper heater section with the test heater for experiments with water and isopropanol (more details in [2]).

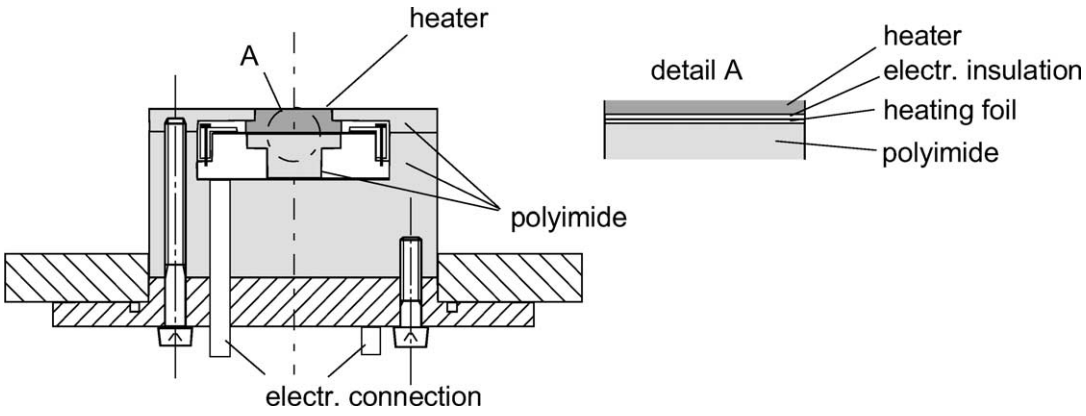

Fig. 3. Experimental setup with test heater No. 2 for FC-72 experiments (more details in [4] and [5]).

The heat input technique for the heaters in Fig. 4 is similar to those of the other heaters (Figs. 2 and 3). A thin heating foil is pressed to the bottom supplied by DC current so that a maximum heat flux of 10 $MW \cdot m^{-2}$ for each heater can be reached. Thin ceramic plates are fixed in the slots between the heaters to reduce axial heat flows. All materials used can cope with temperatures above 1000 °C and the heating foil can be used up to 1400 °C. The heaters are made of copper (5 mm thick) with a nickel layer (0.5 mm thick) on the boiling surface. In each heater 3 thermocouples with 0.25 mm diameter are located along the center line. Two more are installed in heater 2 where the jet impinges. The sensors were electroplated on the surface of the copper base before electroplating the nickel cover.

Model-based heater design. For the design of the described test heaters, several competing and contradicting design criteria have to be considered to allow for a safe operation of the apparatus and to conduct meaningful boiling experiments. To meet these design objectives optimally a model-based design approach has been applied which includes 2- and 3-D FEM simulations of the temperature field and stability analyses of the controlled apparatus. More details of the pool boiling experiments are presented in [2,5, 6].

2.3. Control concept and stability analysis

The wall temperature is controlled by measuring the temperature close to the boiling surface, comparing it to a setpoint value which is either constant in steady-state experiments or time-varying in transient experiments, feeding the difference signal into the controller and adjusting the power of the electric heating according to the controller output. The setpoint signal as well as the control law are

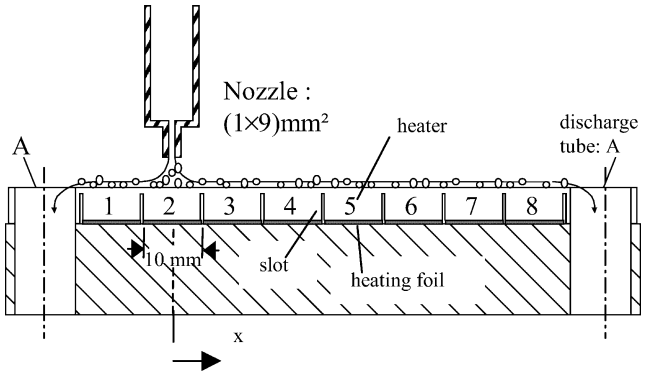

Fig. 4. Outline of the test heater-cascade for jet impingement experiments with water (more details in [1]).

implemented on a computer. More details are presented in [5] for steady-state and the transient experiments with FC-72.

The access to the transition region in the case of water experiments and to a certain extent also in the isopropanol tests, is more difficult than with FC-72 because of the high heat fluxes and the steep negative slope of the boiling curves. A stability analysis has been performed based on the Laplace domain transfer function model of the test heaters, i.e., the one-dimensional heat conduction equation and all control loop elements. Solving for the poles of the closed-loop system numerically, the stability limits of the controlled system can be found. Details of the analysis are described in [6]. For example, in the pool boiling experiments with water, an optimal choice of the P-controller gain allows steady-state measurements of the transition boiling curve with slopes steeper than -9×10^4 W·m^{-2}·K^{-1} [2].

2.4. Data acquisition and measurement evaluation

Water and isopropanol pool boiling experiments. Heating voltage, heating current and amplified temperature signals are sampled with the data acquisition board PC30 (Meilhaus Electronic). For the isopropanol experiments, this card has been replaced by two DoqBoard2000 cards (IOTech). The sampling frequency for each channel is 60 Hz. Data are sampled for 15 s for each point of the boiling curve.

Heater temperature control is realized by the digital signal processing board AT-DSP 2200 (National Instruments). The discrete PI-controller runs on the onboard DSP-processor. The total duration between stimulus and response at the output of the card is 1.5 ms. The input heater temperature used for the temperature controller is the instantaneous average of 4 sheathed thermocouples in the test heater. The output voltage of the card is amplified and supplied to the heating foil.

Heating power is calculated by multiplying heating voltage and current for each data point and then averaged to obtain a point of the boiling curve. The surface superheat is calculated by correcting the time average of the temperature measured by thermocouples by the temperature difference between sensor location and heating surface, assuming onedimensional temperature field in the test heater. The same holds for the steady-state experiments with FC-72.

FC-72 experiments. The same boards are used for data acquisition and control as in the water and isopropanol experiments. In the steady-state case data are sampled for 2 s for each point of the boiling curve. The entire boiling curve is recorded by successively raising or lowering the setpoint value. In transient experiments, the controller must additionally track a prescribed temperature trajectory. Here, a ramp with the temporal gradient as the varied parameter and as a measure for transient dynamics is chosen. The sampling frequency for each channel is chosen to be 200 Hz during steady-state experiments, 500 Hz during slow transients up to 15 K·s^{-1} and 5000 Hz during fast transient runs. In transient experiments, both heat flux and temperature at the heater surface are calculated by means of an inverse heat conduction algorithm presented in [5].

Water jet impingement experiments. The measurements are carried out by setting the mean temperatures of each heater to the same value. The mean temperatures have been increased in steps of 2 or 5 K until film boiling is reached at the stagnation line. Data points for each heater are sampled with a frequency of 200 Hz during 2 s. These data are then used to compute the local temperatures and heat fluxes along the surface of each heater by solving the 2D inverse heat conduction problem. This procedure enables the determination of entire local boiling curves between $x = 0$ (stagnation line) and $x = 55$ mm (see Fig. 4).

2.5. Optical probe

To investigate the liquid-vapor fluctuations above the heater, a fiber-optic probe has been developed. The set-up of the optical probe is based on an earlier development of Auracher and Marroquin [7]. It consists of a gradient index glass fiber with the end of the fiber formed into a conical shape. This is done by melting the tip under a microscope with a small burner. The fiber is then glued into small stainless steel tubes with increasing diameter to make it sufficiently stiff. The probe tip diameter is only 10 μm. The probe can be moved at different heights and different locations above the heater by means of a 3D-micrometer adjusting device (see Fig. 1).

3. Results

3.1. Steady-state pool boiling experiments with FC-72

In Fig. 5, the steady-state boiling curve of FC-72, measured with heater No. 1, is plotted. All experiments were performed with saturated test fluid at a temperature of 333 K which corresponds to a pressure ratio of $p/p_{cr} =$

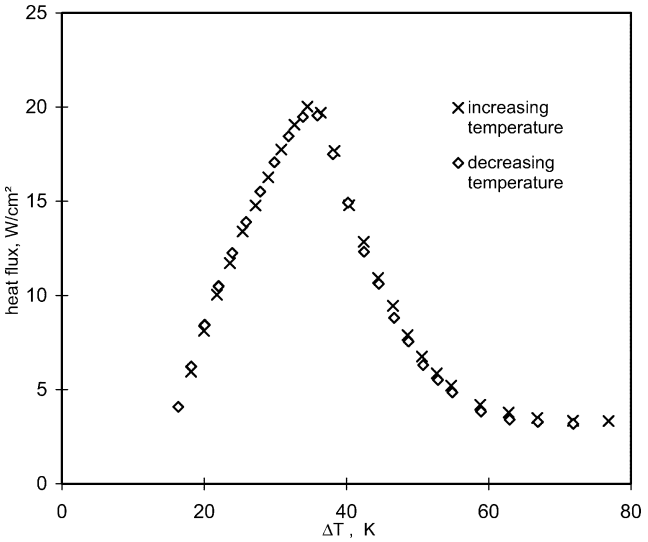

Fig. 5. Steady-state boiling curve of FC-72 measured with heater No. 1; $p = 0.13$ MPa ($p/p_{cr} = 0.071$) (more details in [12]).

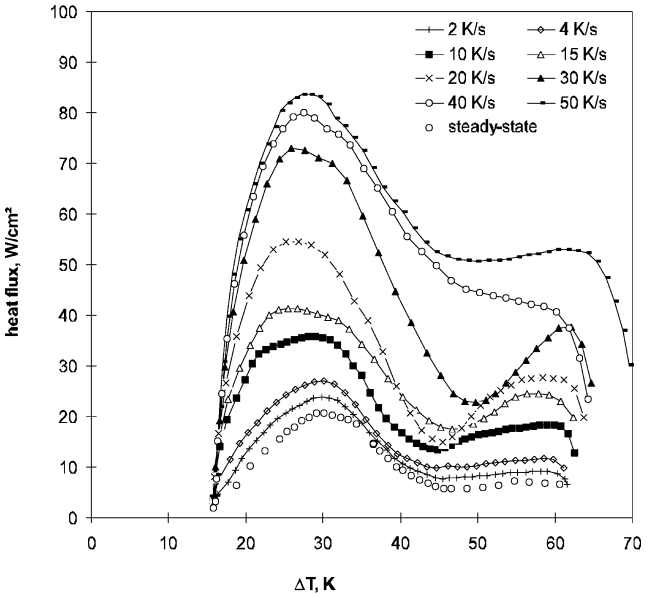

Fig. 6. Boiling curves of FC-72 for transient heating; $p = 0.13$ MPa ($p/p_{cr} = 0.071$) (more details in [5]).

0.071, where p_{cr} denotes the critical pressure (1.83 MPa). The boiling curve in Fig. 5 was measured with stepwise increasing and decreasing heater temperature.

No hysteresis was observed (the well-known hysteresis at inception of boiling was not in the scope of the studies). This result does neither agree with Witte's and Lienhard's [8] assumption of two transition boiling curves nor with the more recent measurements by Ungar and Eichhorn [9]. Reasons for these discrepancies are discussed in former reviews [10,11]. In addition it should be mentioned that contamination during the steady-state experiments can shift the boiling curve. Ungar and Eichhorn mention the build up of a thin black powdery coating on the heating surface during their experiments. Before the final cleaning of our test apparatus we also observed some contamination on the heater during a preliminary experiment. In this case the boiling curve was also not reproducible, neither in steady-state heating nor in steady-state cooling modes. It was furthermore assumed [9] that results from a small heater are not representative because of the similarity of heater diameter and the most dangerous Taylor wavelength and that this effect may explain the discrepancies in the different experiments mentioned above. This is, however, not likely since the diameter of heater No. 1 is 4.3 times larger than the most dangerous Taylor wavelength (7.9 mm for FC-72 at 60 °C). We, therefore, believe that boiling curves measured under steady-state conditions with a proper control and a clean heater surface do not exhibit a hysteresis in the transition boiling region. However one reservation should be made. The contact angle between FC-72 and nickel is small. For clarification, experiments expecially with water are therefore desirable, where the contact angle is significantly larger than with FC-72 (see Section 3.3).

3.2. Transient pool boiling experiments with FC-72

Boiling curves for transient heating. Boiling curves for transient heating with up to 50 $K \cdot s^{-1}$ nominal temperature change per second of the heating surface measured with heater 2 (Fig. 3) are depicted in Fig. 6. These curves represent heat fluxes and temperatures at the heater surface determined by solving the inverse heat conduction problem [5]. For comparison, the steady-state boiling curve is also plotted. Like the boiling curve in Fig. 5, it was measured with stepwise increasing and decreasing temperature and again no hysteresis was observed. This curve deviates a little from the one in Fig. 5. The main reason is that we did not take into account precisely the heat losses of the different heaters. Consequently, some small errors are also included in the determination of the surface temperature. Since these errors have no influence on the qualitative shape of the boiling curves, we made no further correction of the plotted data. All experiments were carried out in a way that nucleation sites were already active at the start of heating (ΔT appr. 15 K) to avoid the disturbance effect of boiling incipience.

Ideally, the slope of the temperature trajectory of the heating surface should be kept constant by the control system during the entire transient period. However, the constant heating rates given in Fig. 6 are nominal values, which deviate slightly from the real ones depending on the transient heating rate. In the first part of the heating period, the surface temperature does not follow precisely the set-point of the control system due to the thermal inertia of the heater. In the subsequent period the effect is vice versa. More details are presented in [5,12].

The heat flux increases strongly with increasing heating rate. At 50 $K \cdot s^{-1}$, the critical heat flux (CHF) is by a factor 4

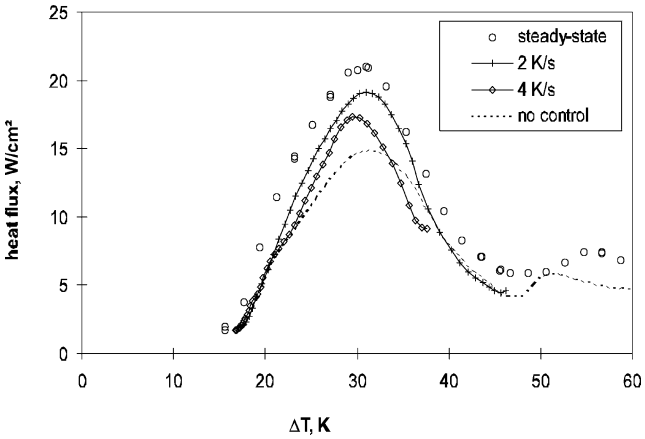

Fig. 7. Boiling curves of FC-72 for transient cooling; $p = 0.13$ MPa ($p/p_{cr} = 0.071$) (more details in [5]).

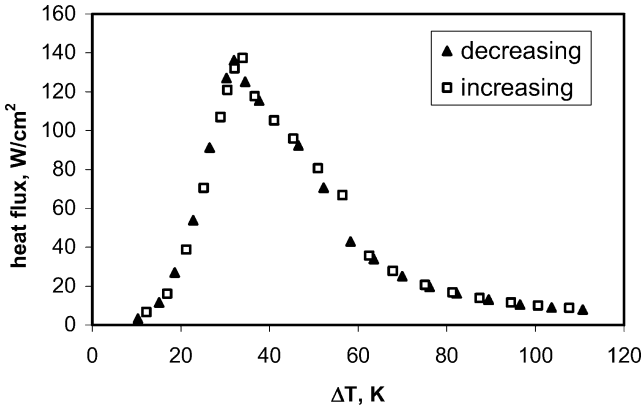

Fig. 8. Boiling curve of distilled water on a clean surface at atmospheric pressure ($p/p_{cr} = 0.0045$).

higher than the one in the steady-state case. The superheat at CHF does not change remarkably with the heating rate. On the other hand, the minimum heat flux of film boiling (MHF) does not exhibit a clear trend. With growing heating rates, it moves first to smaller and than to higher superheats. In some transients, no distinct minimum is observed. The heat flux in film boiling during the heating mode is significantly higher than in steady-state heating. After switching off the heating power to start the cooling mode somewhere between a superheat of 60 and 70 K the heat flux drops down to at least the value of the steady-state case (see Fig. 7).

It can easily be proven that the behavior shown in Fig. 6 is not due to an evaluation uncertainty or error. An energy balance reveals that the total heat input during the heating period between nucleate and film boiling is equal to the one accumulated in the heater plus the heat supplied to the fluid, which follows from an integration of the transient boiling curve over time. An estimate shows that the error due to the storage of heat in the insulation around the heater is negligibly small. Hence, the following conclusions can be drawn:

(1) the inverse heat conduction problem is solved properly, and
(2) the boiling curve characteristic in transient heating shown in Fig. 6 is due to a physical effect of the boiling mechanism.

Boiling curves for transient cooling. Due to the thermal inertia of the heater the cooling rate is limited. Constant cooling rates were only possible for 2 $K{\cdot}s^{-1}$ along the entire boiling curve and for 4 $K{\cdot}s^{-1}$ between transition and nucleate boiling (see Fig. 7). With zero heat input, the cooling rate was about 2 $K{\cdot}s^{-1}$ in film boiling and 6.8 $K{\cdot}s^{-1}$ in the CHF-region. Obviously, the transient cooling effect is contrary to the transient heating behaviour (notice that the steady-state curve in Fig. 7 is the same as the one in Fig. 6). The faster the cooling rate the smaller the heat flux. A key to a physical explanation of the transient boiling mechanism is given by the data obtained from the optical probe and from the temperature fluctuations on the heating surface discussed later in this report.

3.3. Steady-state pool boiling experiments with water and isopropanol

Water. The experiments with water were performed at atmospheric pressure ($p/p_{cr} = 0.0045$). Before conducting an experiment, the system was evacuated and then heated up with the thermostatic bath and the steam generator to saturation temperature. After reaching atmospheric pressure in the system, a valve to the atmosphere was opened and the cooling liquid for the condenser was turned on. To prevent oxygen from entering the system, excess Argon was supplied to the top of the condenser throughout the experiments.

Fig. 8 shows the boiling curve for distilled water on a clean surface. The boiling curve was measured with stepwise decreasing temperature from a starting point in the film boiling regime to low heat flux nucleate boiling. Afterwards, the heater temperature was increased stepwise starting in nucleate boiling until film boiling was reached again. The heater temperature control was able to stabilize the boiling process in all boiling regimes. All points of the boiling curve were measured under steady-state conditions. The two boiling curves (in Fig. 8) are almost identical. No distinct hysteresis in the transition boiling regime can be identified. However, a small disturbance in the shape of the otherwise smooth curve is recognizable at a ΔT of about 55 K in Fig. 8. A similar but even smaller effect can be observed in the transition boiling region of isopropanol at $\Delta T \approx 40$ K (Fig. 10). There are indications that non-uniform boiling effects may cause these slight alterations of the boiling curve shape. We may have larger clusters of dry patches on the surface which possibly change their configuration with the wall superheat leading to the above mentioned disturbances. The size of the clusters is still much smaller than the heater surface area but they are large enough to disturb the ergodic behavior of the boiling mode across the surface. In our

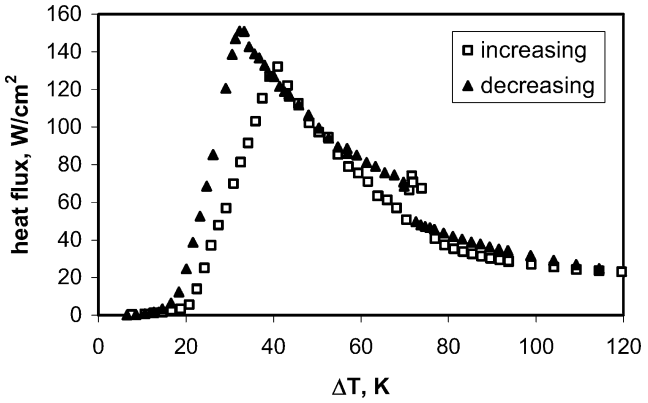

Fig. 9. Boiling curve of power station feedwater on a surface with deposits at atmospheric pressure ($p/p_{cr} = 0.0045$) (more details in [2]).

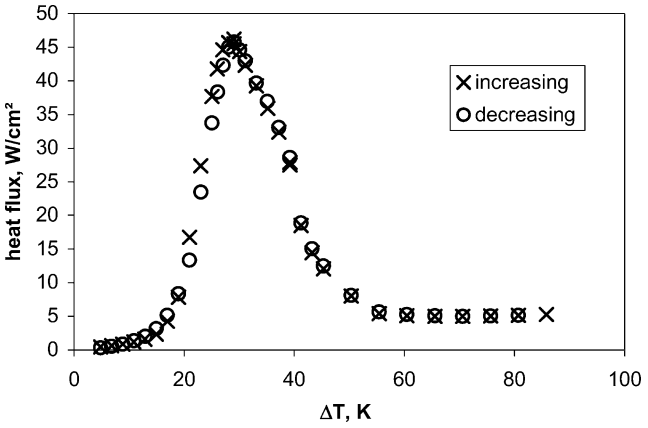

Fig. 10. Boiling curve of isopropanol at 0.12 MPa ($p/p_{cr} = 0.025$).

measurements with FC-72 we did not observe this kind of disturbances. We are not yet able to give a physical explanation for this effect. It is subject of current studies.

Fig. 9 shows boiling curves for power station feedwater on a surface with deposits. The experiment was performed before the experiment presented in Fig. 8. Unlike the boiling curve in Fig. 8, this boiling experiment was conducted in the opposite direction. After approximately 30 s boiling at CHF to activate the nucleation sites on the heater and a subsequent decrease of the wall temperature, the heater temperature was increased stepwise from nucleate to film boiling and back vice versa. The shape of the boiling curve changed significantly during the experiment.

Mostly, the boiling curve shifts to higher heat fluxes and the superheat at CHF decreases. The effect is similar to that one observed by Ungar and Eichhorn [9]. The boiling surface changed remarkably during our experiment. An opaque layer of a white, hard substance built up on the surface. The layer could not be removed with solvents or citric acid. Therefore it was removed by emery paper P2000 to achieve an identical finish of the surface for the next experiment.

The hysteresis in Fig. 9 is not a result of insufficient reproducibility caused by the experimental facility itself. Measurements within the nucleate boiling region up to CHF show excellent reproducibility. No buildup of deposits could be identified during these tests. Deposits on the heater are more likely to build up during extremely rapid local evaporation at the heater surface as it is the case in transition boiling. In fact, this could be observed during many previous tests. Reducing all possibilities which may lead to deposits, e.g., insufficient purity of the test liquid, long measurement duration, insufficient filtering of the test liquid etc., to a minimum, leads to the boiling curves as the one plotted in Fig. 8. In this case, as mentioned before, we changed the experimental scheme and started in film boiling. Assuming the speed of deposition to be maximal in transition boiling and to be less in the film boiling region, this scheme leads to minimal influence of deposits in the nucleate boiling curve. In fact, only small differences between the boiling curves measured with increasing and decreasing wall temperatures can be seen in Fig. 8. In summary all our results let us conclude that with ultra clean surfaces and fluids the transition region exhibits no systematic hysteresis irrespective of the sequence of the measurement. However, effects as mentioned in the second paragraph of the present chapter may affect the transition boiling curve.

At this stage of the investigation, an influence of controller action on the boiling process and therefore on the boiling curve can not completely be excluded. The maximum mean heater temperature fluctuations observed in transition boiling were 3 K. These fluctuations are most likely caused by extremely high local heat fluxes during dry-out/rewetting periods on the surface, but they may influence the boiling process by controller action. This point will be further investigated in the future. Incidentally, the most dangerous Taylor wavelength is 19 mm for boiling water at atmospheric pressure and thus, as in the FC-72-experiments, much smaller than the heater diameter.

Isopropanol. The tests with isopropanol were carried out in a pressure range between 0.033 MPa ($p/p_{cr} = 0.007$) and 0.332 MPa ($p/p_{cr} = 0.07$). Hence, the system was—in contrast to the water experiments—closed to the atmosphere. As with the other fluids reproducible boiling curves could only be obtained with a carefully purified liquid and a clean surface. In this case again no hysteresis was observed between curves measured with stepwise increasing temperature and stepwise decreasing temperature, respectively. An example is shown in Fig. 10.

3.4. Steady-state jet impingement experiments with water

Fig. 11 presents local boiling curves at a jet velocity of 0.8 $m \cdot s^{-1}$, a subcooling of 16 K and a distance between nozzle and surface of 6 mm, for the stagnation line ($x = 0$) and $x = 19$ and 44 mm, respectively (see Fig. 4). The boiling curve in the stagnation line is different from the ones measured in the parallel flow region. At the stagnation line the transition boiling regime occupies a large range of

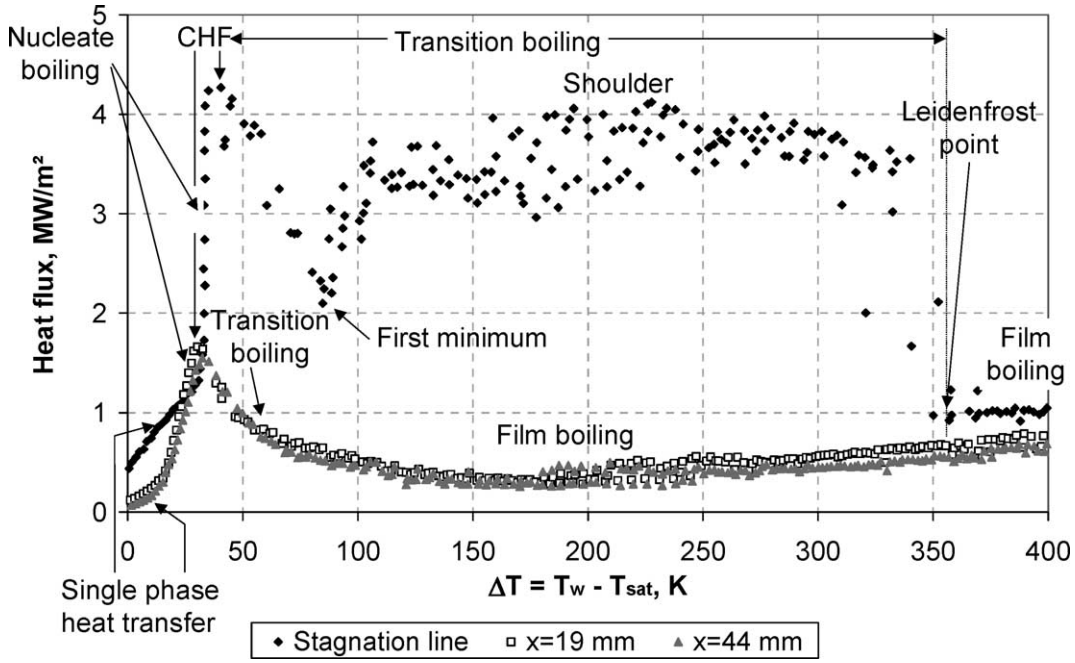

Fig. 11. Local boiling curves at jet impingement cooling with water ($p = 0.1$ MPa, $p/p_{cr} = 0.0045$). Jet velocity: 0.8 m·s^{-1}, subcooling: 16 K, distance between nozzle and surface: 6 mm (more details in [1]).

superheats and the corresponding heat flux is almost as large as the critical heat flux under the given system conditions. In contrast, boiling curves in the parallel flow region are similar to the classical ones obtained for forced convection boiling.

In the single phase heat transfer regime, the heat flux decreases as the distance from the stagnation line increases, certainly because the boundary layer thickness increases downstream. With rising wall superheat nucleation first starts away from the stagnation line. All our experiments (more details in [1]) clearly indicate that the smaller the distance to the stagnation line the higher the superheat at onset of nucleation. CHF is first reached in the parallel flow region. There, it occurs at about the same superheat when onset of nucleation is observed at the stagnation line. In the present system conditions CHF is about three times larger at the stagnation line than in the parallel flow region.

At the stagnation line, after CHF, the heat flux decreases with increasing superheat as in classical pool or convective boiling systems. However, at a superheat of about 80 K the curve exhibits a minimum and the heat flux starts to increase again. A similar phenomenon has already been reported by Torikai et al. [13] and Suzuki et al. [14]. They interpret this effect as the beginning of the so-called microbubbles emission boiling. The authors assume that bubbles break into many microbubbles which induces a local mixing of the fluid leading to a better wetting of the surface and, hence, a better heat transfer. In [13,14] the heat flux decrease between CHF and the first minimum could not be measured as a heat flux controlled system was used. The following might happen in this region: after CHF the surface wetting is characterized by very small vapor spots as a result of bubble coalescence. Hence, the overall heat flux is smaller than at CHF where fewer vapor spots exist. As the vapor spots grow towards the first minimum the heat flux decreases. In this region with a negative slope the jet energy is not high enough to break the vapor spots. This may, however, take place at superheats above the one at the first minimum, where the vapor spots are now large enough to be broken down by the jet. The result would be a better—spray type—wetting of the surface leading to higher heat fluxes. The above explanation would become plausible if at higher jet velocities, and thus at an increased ability to break the vapor spots, the part between CHF and the first minimum would step by step disappear with increasing jet velocity. In fact, in some experiments with higher velocities we observed this trend.

With a further wall temperature increase the ability of the liquid to wet the surface decreases. Consequently, the overall area of liquid contact decreases. In these smaller contact areas, however, the heat fluxes are higher than in the contact zones at lower wall temperatures. As a result the overall heat flux remains appr. constant (shoulder, Fig. 11), though due to the explosive boiling character at these high temperatures strong heat flux variations are observed.

At a wall superheat of about 350 K, the heat flux beneath the jet decreases nearly abruptly and the surface dries out. At $x = 0$ the Leidenfrost temperature is about 250 K higher than in the parallel flow region. It rises strongly with increasing subcooling [1] and the jet velocity has a similar effect. In film boiling the heat flux is about 25% larger at the stagnation line than in the parallel flow region, most likely because the vapor film on the heating surface becomes thicker downstream.

3.5. Experiments with the optical probe and FC-72

These experiments have been carried out with heater No. 1 under steady-state conditions. Three series of measurements were carried out, one with the probe tip at the heater center, a second one 8 mm from the center and a third one 15 mm from the center. It was found that no significant difference exists between the probe signals from different locations, indicating homogeneous boiling conditions on the heater surface. Measurements were carried out at distances of the probe tip from the heater surface of 0.01, 0.03, 0.05, 0.1, 0.5 and 1 mm. The distance was determined with an accuracy of ± 0.01 mm by measuring the signal rise as a result of light reflexion at the heater surface when the probe comes very close to it. In measurements at 0.01 mm nominal distance from the heater, it can be assured that the probe tip was fixed within a real distance between 0.005 mm and 0.02 mm from the heater surface. For more details of the probe experiments see [3,12].

In Fig. 12 the void fraction measurements above the heater center are plotted against the distance from the heater surface. For nucleate boiling up to CHF ($\Delta T = 20$ K to $\Delta T = 35$ K) the void fraction decreases sharply when the probe comes to the heater surface. This can also be observed at $\Delta T = 40$ K in the transition boiling regime. The existence of a liquid rich layer near the heater surface, the so-called macrolayer, is therefore confirmed. The macrolayer thickness decreases with increasing heater temperature. The location of the maximum void fraction above the heater is found to be at about 0.5 mm in nucleate boiling, at 0.1 mm at CHF, at 0.05 mm at $\Delta T = 40$ K and it reaches the heater surface at $\Delta T = 50$ K.

The results are in general agreement with results of Iida and Kobayasi [15] and Shoji [16]. But the measured thicknesses of the liquid rich layer above the heater surface in the present investigation, with FC-72, are far smaller than those in the above cited references. As in these investigations water was used as test fluid data cannot be compared quantitatively. If the data in Fig. 12 are extrapolated to the heater surface, which certainly implies some error, a continuous increase of the non-wetted fraction is observed with increasing wall temperature from nucleate to film boiling. The non-wetted fraction at CHF is, e.g., less than about 15%.

Fig. 13 shows the mean vapor contact frequency at the probe tip. The number of vapor contacts increases when the probe is moved towards the heater surface and reaches frequencies as high as 500 to 600 Hz at about 0.05 mm from the heater surface. It seems that at about these distances the probe detects bubbles from several nucleation sites during their growing period. At larger distances the bubbles coalesce to bigger vapor masses resulting in a decrease of the frequency. A further approach of the probe tip to the surface results in a decrease of the frequency. An explanation could be that at these very small distances the probe tip touches less and less bubbles during their growing period probably

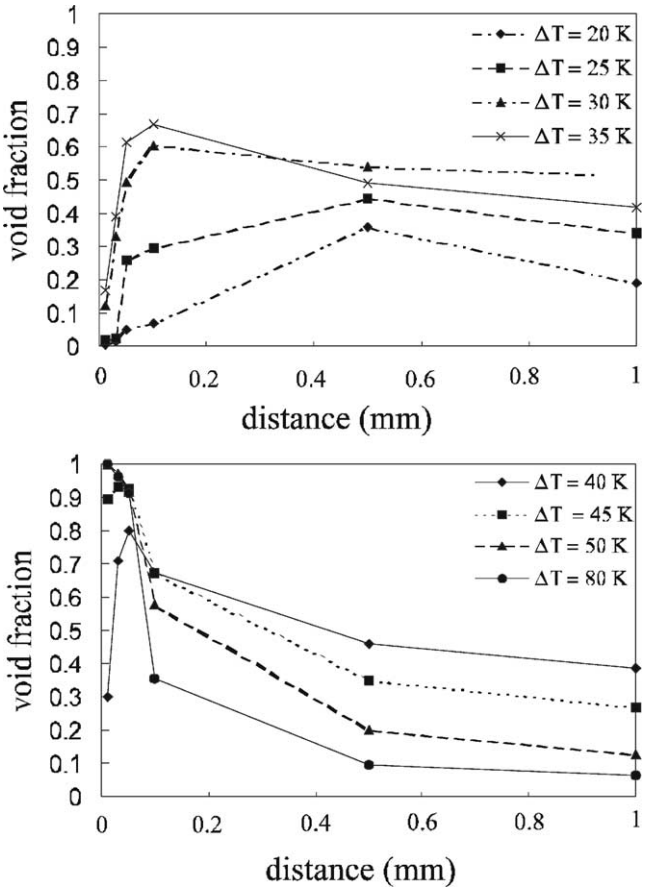

Fig. 12. Time averaged void fraction; FC-72; heater No. 1 (more details in [3,12]).

at most two if we look at the detected frequency of less than 100 Hz.

In transition boiling liquid contacts during a "wetting period" become so short that it is not possible to clearly detect all of them. Consequently the liquid contact frequency and therefore as well the vapor contact frequency is underestimated. Here it is more reasonable to look at the distribution of the vapor detection frequency and the distribution of vapor and liquid contact times as presented in [3].

In transient boiling the probe measurements were not successful due to the unavoidable thermal expansion and contraction of both the probe and the heater. It turned out that during a transient run the distance between the probe tip and the heater surface varied within a range where the strongest changes in contact frequencies and other quantities occur.

3.6. Experiments with microthermocouples and FC-72

For a further insight into the liquid/vapor behavior at the heating surface experiments with microthermocouples embedded at a small distance to the surface (appr. 20 μm) have been carried out with heater No. 2 (Fig. 3). The objective was to extract some conclusions on the mechanism of boiling in the different boiling regimes from the measured temperature fluctuations, especially to explain the strong

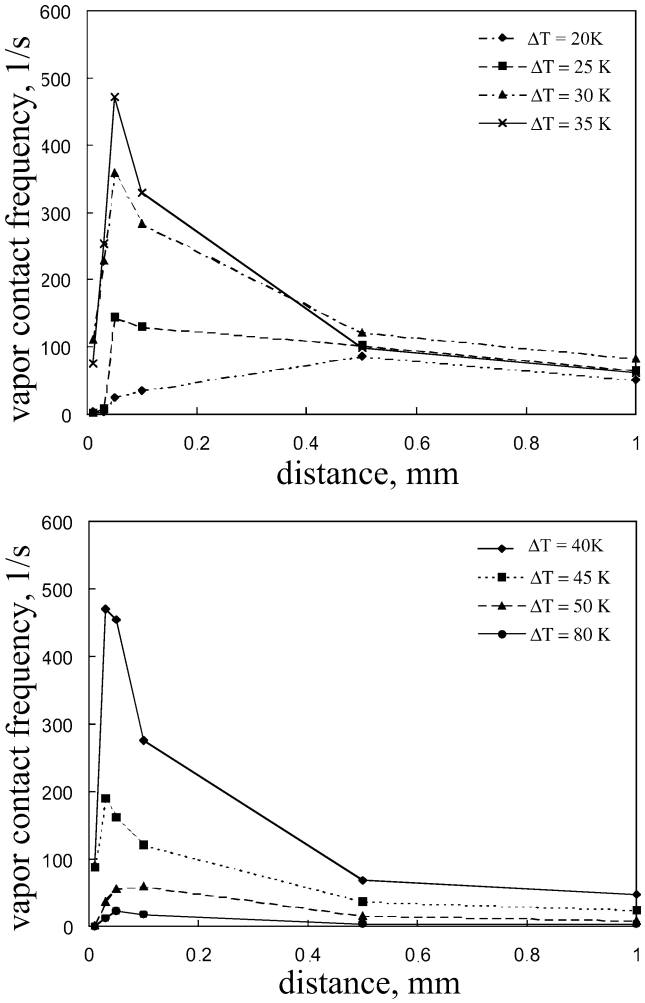

Fig. 13. Mean vapor contact frequency at the optical probe tip; FC-72; heater No. 1 (more details in [3,12]).

difference between steady-state and transient data. Details of these measurements are presented in [4,12]. Standard statistical analyses of the temperature fluctuations led us to the following conclusions:

Up to CHF no difference in signal characteristics occurring at a given wall superheat in steady-state or transient runs is observed. If the wall superheat increases further the temperature amplitudes also increase but now a delay in amplitude amplification can be observed in transient runs, i.e., in the transition region the instantaneous temperature amplitudes at a given wall superheat are smaller in transient runs than in a steady-state measurement. An analogous conclusion holds probably for the cooling mode, however, the transients were not fast enough for a clear observation of this rather small effect. Our preliminary conclusion is therefore—under the reservation that the presently available number of data are not high enough for a well established statistical statement—that no significant difference in the wetting mechanisms exists under steady-state and transient conditions at the same wall superheat up to about CHF. Beyond CHF, however, a delay effect in the liquid-vapor fluctuations seems to occur. Hence, in transient heating the two-phase structure formation above the heating surface may not be sufficiently fast to follow a fast transient.

The above conclusion for the nucleate boiling region is not surprising. Assume the bubble departure frequency to be 100 Hz. Then, during the period between two bubbles, the temperature rise of the heater surface is only 0.5 K at the fastest transient of 50 $K{\cdot}s^{-1}$ (Fig. 6). Hence in a first approach we may argue that since vapor generation and wetting mechanism are much faster processes than the change of the average temperature with time during a transient, the vapor/liquid structure close to the heater surface region for a given ΔT is not strongly influenced by the transient. It is therefore acceptable to rely also on the steady-state optical probe results if we search for a physical explanation of the heat transfer behavior in transient nucleate boiling up to CHF.

4. Conclusions

Based on all the presented experimental results the following conclusions on the behavior of boiling curves and on the mechanisms of heat transfer in the nucleate boiling region and in boiling regimes with higher wall superheat can be drawn.

4.1. Boiling curves

Under steady-state pool boiling conditions with a good control system to stabilize boiling in the transition region, and a clean heater surface, no hysteresis has been observed in the transition region for both well wetting fluids and fluids with a larger contact angle. Small disturbances in the transition boiling curve have been observed with water and isopropanol. This may result from a non-ergodic boiling behavior on the heater surface. For a surface with contamination, boiling curves are not reproducible. Under transient conditions a hysteresis is observed: heating transients yield always higher heat fluxes than cooling transients at the same wall temperature. At fast transients enormous differences in the heat fluxes compared with the steady-state case have been observed.

In jet impingement the boiling curves behave classicly outside of the stagnation region. In the center of the jet, however, their shape is significantly different from classical boiling curves: the CHF is by some factors (depending on subcooling and jet velocity) larger than in pool boiling. The transition region occupies a larger range of superheats and the corresponding heat flux is in a similar order of magnitude as CHF (at the system conditions used here: $\Delta T_{\mathrm{sub}} = 16$ K, $v = 0.8\ \mathrm{m{\cdot}s^{-1}}$). At relatively very high wall superheats (here appr. 350 K) the heat flux decreases nearly abruptly and a vapor film beneath the jet forms. In film boiling the heat flux is about 25% larger at the stagnation line than in the parallel flow region.

4.2. The structure of the macrolayer

The existence of a liquid-rich layer, the so-called macrolayer, has been proven in the experiments. With FC-72 the thickness of this layer decreases with increasing heater temperature from about 0.5 mm in nucleate boiling to 0.1 mm at CHF until it disappears in the transition boiling region. The assumption of stationary vapor stems in the macrolayer is rather unlikely as only very short vapor contacts of at most 5 to 10 ms duration were detected close to the heater (more experiments of this kind are presented in [3]). Instead in the high heat-flux region the state of the two-phase flow in the macrolayer-region is quite agitated. At a distance of 0.05 mm from the heater up to 600 vapor contacts per second were measured. Activation of nucleation sites does not exhibit regularity and takes place in a wide frequency band.

4.3. Nucleation site densities

A comparison of probe signals (Figs. 12 and 13) and microthermocouple signals [4,12] enables an estimate of the density of active nucleation sites. It turns out, e.g., that the minimum nucleation site density near CHF is about 3×10^8 per m^2. Regarding the uncertainty of this estimate we may conclude that the nucleation site density is between 10^8 and 10^9 per m^2. This is in the order of magnitude of the results of Pinto et al. [17] who observed 4×10^7 nucleation sites per m^2 in propane boiling at a heat flux of 5 $W \cdot cm^{-2}$, which is below CHF.

4.4. Some qualitative conclusions on the mechanism of heat transfer in different boiling regimes

Pool boiling. The high density of active nucleation sites in the region between fully developed nucleate boiling and CHF and the resulting highly turbulent two-phase boundary layer let us conclude that the strong increase of heat flux in heating transients and vice versa in a cooling process is mainly due to the intensive two-phase convection heat transfer from the wall to the bulk. Note that this is most likely not primarily because of a change in the two-phase structure (i.e., nucleation site density, bubble frequency, void fraction distribution etc.) near the wall, which is not significantly affected by temperature transients. Rather, it is mainly due to the instantaneous temperature gradient in the fluid at the heater surface which is increased or decreased during the transient modes. Hence, the highly turbulent microconvective transfer of energy is intensified if it takes place in a temperature field with steeper gradients caused by transient heating or with weaker gradients in the cooling mode. Clearly, at this stage we have no direct experimental indication for steeper or weaker temperature gradients during the transients. Furthermore our measurements of the two-phase structure near the wall and its behavior during transients are not precise enough to exclude an error in the above statement. Therefore, more precise measurements along the line presented in this report should be carried out to support this conclusion. Besides, an estimate reveals that unsteady-state heat conduction to the liquid cannot explain the strong increase of heat flux during a heating transient.

The results obtained with microthermocouples [4,12] let us furthermore assume that at wall superheats beyond CHF the two-phase structure at a given wall superheat is not independent of the heating or cooling rate. The faster the transient the stronger the delay in the two-phase structure formation. This could be one reason for the deviation of heat flux between the transient and steady-state case in the transition and film boiling region. But we need more experiments with our microsensors to gain a better insight in the physics responsible for this deviation.

Jet impingement boiling. In the stagnation region of a jet, the boiling mechanism is similar to pool boiling or forced convection boiling except for the transition region, but the heat fluxes are significantly larger. In the transition region it seems that the jet destroys the larger vapor spots leading to a spray type wetting and hence to very large heat fluxes up to high wall superheats. Then film boiling starts rather abruptly.

4.5. Needs for further studies

Our experiments provide a deeper insight in some aspects of the extremely complex mechanisms of boiling. But many aspects are still not clearly understood or even unknown in this field. However, there is a high potential for more precise and new experimental results by improving our experimental tools. A further miniaturization of thermocouples implanted extremely near to the surface by galvanotechniques is required. In addition the optical probes should also be miniaturized and used in a multiple arrangement. Simultaneous measurements with these improved sensors should yield a clearer picture of the two-phase behavior on and above the heater surface and the resulting temperature field inside the heater. These are key data for the development of mechanistic models for boiling in the different regimes. With a proper control system it is no problem to fix any state along the boiling curve as long as we like.

Of course, other types of experiments are also required, e.g., using modern optical techniques, and last but not least we need approaches by theoretical studies. Substantial progress is only possible if we tackle the problem from both the experimental and the theoretical end. Preferably, both approaches should be closely linked.

We studied here only boiling-phenomena on smooth surfaces. Heat transfer enhancement by structuring the surfaces has already a long history. Most of the basic phenomena occurring at smooth surfaces are also relevant at enhanced surfaces, but several additional problems have to be solved in these cases. Last but not least, in practical applications we have quite often boiling mixtures which bring some more parameters to be studied into the game. In

summary there is still a lot to do but real progress requires studies of the fundamentals.

Acknowledgements

We would like to acknowledge the financial support of the "Deutsche Forschungsgemeinschaft (DFG)" and we also thank 3M Deutschland GmbH for providing us with the test fluid FC-72. Furthermore we are grateful to J. Blum, M. Buchholz, R. Hohl, T. Lüttich, H. Robidou who developed the results presented here in the frame of their Ph.D. Theses.

References

[1] H. Robidou, H. Auracher, P. Gardin, M. Lebouché, Controlled cooling of a hot plate with a water jet, in: Proc. 5th World Conf. On Exp. Heat Transfer, Fluid Mechanics and Thermodynamics, Thessaloniki, September 24–28, 2001.

[2] M. Buchholz, T. Lüttich, H. Auracher, W. Marquardt, Steady state pool boiling experiments with water between nucleate and film boiling, in: Proc. 3rd Europ. Thermal Sciences Conf. 10–13 September, Heidelberg, Germany, 2000, Paper 3–10.

[3] R. Hohl, H. Auracher, J. Blum, W. Marquardt, Characteristics of liquid-vapor fluctuations in pool boiling at small distances from the heater, Heat Transfer 1998, Proc. 11th Internat. Heat Transfer Conf. 1 (1998) 383–388.

[4] R. Hohl, H. Auracher, Transient pool boiling experiments, in: F. Mayinger, B. Giernoth (Eds.), Transient Phenomena in Multiphase and Multicomponent Systems, Wiley-VCH-DFG, 2000, pp. 241–256.

[5] R. Hohl, J. Blum, M. Buchholz, T. Lüttich, H. Auracher, W. Marquardt, Model-based experimental analysis of pool boiling heat transfer with controlled wall temperature transients, Internat. J. Heat Mass Transfer 44 (2001) 2225–2238.

[6] J. Blum, W. Marquardt, H. Auracher, Stability of boiling systems, Internat. J. Heat Mass Transfer 39 (1996) 3021–3033.

[7] H. Auracher, A. Marroquin, A miniaturized optical sensor for local measurements in two-phase flow, in: Proc. 10th Brazilian Congr. of Mech. Engng., Rio de Janeiro, 1989, pp. 13–16.

[8] L.C. Witte, J.H. Lienhard, On the existence of two transition boiling curves, Internat. J. Heat Mass Transfer 25 (1982) 771–779.

[9] E.K. Ungar, R. Eichhorn, Transition boiling curves in saturated pool boiling from horizontal cylinders, J. Heat Transfer 118 (1996) 654–661.

[10] H. Auracher, Transition boiling, in: Heat Transfer 1990, Proc. 9th Internat. Heat Transfer Conf., Vol. 1, 1990, pp. 69–90.

[11] H. Auracher, Transition boiling in natural convection systems, in: V.K. Dhir, A.E. Bergles (Eds.), Pool and External Flow Boiling, Engng. Foundation, 1992, pp. 219–236.

[12] R. Hohl, Mechanismen des Wärmeübergangs beim stationären und transienten Behältersieden, in: VDI Fortschritt-Berichte, Vol. 3/597, VDI, Düsseldorf, 1999.

[13] K. Torikai, K. Suzuki, A. Suzuki, T. Watanabe, Microbubbles emission in subcooled transition boiling by use of multi-water-jet, in: Proc. 3rd Internat. Sympos. On Multiphase Flow and Heat Transfer, Xi'an, China, 1994, pp. 70–77.

[14] K. Suzuki, K. Saito, T. Sawada, K. Torikai, An experimental study on microbubble emission boiling of water, in: Proc. 3rd Europ. Thermal Sciences Conf., Heidelberg, Germany, 2000, pp. 815–820.

[15] Y. Iida, K. Kobayasi, An experimental investigation on the mechanism of pool boiling phenomena by a probe method, in: Heat Transfer 1970, Proc. 4th Int. Heat Transfer Conf., Vol. 5, B 1.3., 1970.

[16] M. Shoji, A study of steady transition boiling of water: Experimental verification of macrolayer evaporation model, in pool and external flow boiling, in: V.K. Dhir, A.E. Bergles (Eds.), Engng. Foundation, 1992, pp. 237–242.

[17] A. Pinto, D. Gorenflo, W. Künstler, Heat transfer and bubble formation with pool boiling of propane at a horizontal copper tube, in: Proc. 2nd Europ. Therm. Sci. Conf., ETS Pisa, Vol. 3, 1996, pp. 1653–1660.